Journal of Heredity, 2023, **XX**, 1–17
https://doi.org/10.1093/jhered/esad046
Advance access publication 27 July 2023
Original Article

Original Article

Species differences in hormonally mediated gene expression underlie the evolutionary loss of sexually dimorphic coloration in *Sceloporus* lizards

Christopher D. Robinson[1], Matthew D. Hale[1,2,3], Tyler N. Wittman[1], Christian L. Cox[4], Henry B. John-Alder[5] and Robert M. Cox[1]

[1]University of Virginia, Department of Biology, Charlottesville, VA, United States,
[2]U.S. Military HIV Research Program, Walter Reed Army Institute of Research, Silver Spring, MD, United States,
[3]Henry M. Jackson Foundation for the Advancement of Military Medicine Inc., Bethesda, MD, United States,
[4]Florida International University, Department of Biological Sciences and Institute of Environment, Miami, FL, United States,
[5]Rutgers University, Department of Ecology, Evolution, and Natural Resources, New Brunswick, NJ, United States

Address correspondence to C.D. Robinson at the address above, or e-mail: cdr4ua@virginia.edu.

Corresponding Editor: Anne Bronikowski

Abstract

Phenotypic sexual dimorphism often involves the hormonal regulation of sex-biased expression for underlying genes. However, it is generally unknown whether the evolution of hormonally mediated sexual dimorphism occurs through upstream changes in tissue sensitivity to hormone signals, downstream changes in responsiveness of target genes, or both. Here, we use comparative transcriptomics to explore these possibilities in 2 species of *Sceloporus* lizards exhibiting different patterns of sexual dichromatism. Sexually dimorphic *S. undulatus* develops blue and black ventral coloration in response to testosterone, while sexually monomorphic *S. virgatus* does not, despite exhibiting similar sex differences in circulating testosterone levels. We administered testosterone implants to juveniles of each species and used RNAseq to quantify gene expression in ventral skin. Transcriptome-wide responses to testosterone were stronger in *S. undulatus* than in *S. virgatus*, suggesting species differences in tissue sensitivity to this hormone signal. Species differences in the expression of genes for androgen metabolism and sex hormone-binding globulin were consistent with this idea, but expression of the androgen receptor gene was higher in *S. virgatus*, complicating this interpretation. Downstream of androgen signaling, we found clear species differences in hormonal responsiveness of genes related to melanin synthesis, which were upregulated by testosterone in *S. undulatus*, but not in *S. virgatus*. Collectively, our results indicate that hormonal regulation of melanin synthesis pathways contributes to the development of sexual dimorphism in *S. undulatus*, and that changes in the hormonal responsiveness of these genes in *S. virgatus* contribute to the evolutionary loss of ventral coloration.

Key words: androgen receptor, evolutionary endocrinology, melanophore, pigmentation, sexual dichromatism, testosterone, transcriptome

Introduction

Although female and male conspecifics share the vast majority of their genomes, differential regulation of transcription can result in the development of remarkably different phenotypes in each sex (Waxman and O'Connor 2006; Mank 2009; Williams and Carroll 2009; Cox et al. 2015, 2017; Wright et al. 2019; Gazda et al. 2020; Khalil et al. 2020). In vertebrates, estrogens and androgens are produced primarily in the gonads and then circulate to target tissues, where they bind nuclear receptors and thereby influence gene expression by interacting with hormone response elements in the genome. Consequently, sex differences in the production of estrogens and androgens lead to sex differences in gene expression, which in turn lead to the development of sexually dimorphic traits (Rinn and Snyder 2005; van Nas et al. 2009; Xu et al. 2012; Frankl-Vilches et al. 2015; Cox et al. 2017; Anderson et al. 2020; Ansai et al. 2021; Hale et al. 2022). Phenotypic responses to steroid hormones can evolve, such that different populations or species exhibit unique responses to the same hormonal stimulus (Cox and John-Alder 2005; Hau 2007; Rosvall et al. 2016; Lipshutz et al. 2019; Blázquez et al. 2020; Anderson and Jones 2022; Enbody et al. 2022). This evolutionary lability can reflect multiple mechanisms, including upstream changes in the sensitivity of target tissues to hormonal signals (e.g. changes in hormone receptor expression) or downstream changes in the responsiveness of specific genes and pathways to the activated hormone receptor (Cox et al. 2022). However, data directly linking evolutionary changes in phenotypes to differences in the hormonal regulation of underlying genes are generally lacking. To provide such data, we combined comparative transcriptomics and hormone manipulations in 2 closely related species representing ancestral (sexually dimorphic) and derived (monomorphic) states for coloration (Ossip-Drahos

Received April 19, 2023; Accepted July 24, 2023

et al. 2016). We use this framework to test whether the evolutionary loss of hormonally regulated sexual dimorphism occurs through upstream changes in tissue sensitivity to a hormonal signal, downstream changes in the responsiveness of specific genes and pathways to a hormonal signal, or a combination of these mechanisms.

Fence and spiny lizards (genus *Sceloporus*) provide an ideal comparative system because they exhibit repeated evolutionary transitions in sexual dimorphism for traits such as body size and coloration (Wiens 1999; John-Alder and Cox 2007; Ossip-Drahos et al. 2016; Jiménez-Arcos et al. 2017). The effects of testosterone on color and growth phenotypes are known to differ across species with different patterns of dimorphism (Quinn and Hews 2003; Cox and John-Alder 2005; Cox et al. 2005a,b, 2007, 2009). For example, *S. undulatus* males have vibrant blue and black patches on their abdomens and throats, whereas this coloration is absent or greatly reduced in females (Fig. 1). These patches can be induced by exogenous androgens in juveniles of both sexes, but they only develop naturally in males due to organizational effects of rising testosterone levels during maturation (Cox et al. 2005a; Pollock et al. 2017), and activational effects of elevated testosterone during the breeding season are required to maintain vibrant blue color in adults (Cox et al. 2005a; Robinson and Gifford 2019). Conversely, *S. virgatus* males do not develop abdominal coloration naturally or in response to exogenous testosterone (Abell 1998b; Quinn and Hews 2003) and their white abdomens are virtually indistinguishable from those of females (Fig. 1). Whereas many *Sceloporus* species have independently evolved a derived state of vibrant ventral coloration in females, suggesting cross-sexual transfer (West-Eberhard 2003; Anderson and Falk 2023), *S. virgatus* has instead lost the ancestral state of vibrant ventral coloration in males that is retained by *S. undulatus*. These 2 species diverged approximately 12 million years ago (Wiens 1999; Ossip-Drahos et al. 2016) and adult males of both species have similarly high levels of circulating testosterone during the breeding season (Abell 1998a; Cox and John-Alder 2005, 2007; Cox et al. 2005a; John-Alder et al. 2009; Hews et al. 2012). Therefore, the evolutionary loss of blue ventral coloration in *S. virgatus* males is due to the loss of color production, either generally or specifically in response to testosterone, rather than a change in circulating testosterone as a signal mediating sexual dichromatism. However, it is unknown whether this loss of color production in *S. virgatus* has occurred via the upstream loss of tissue sensitivity to testosterone, via downstream changes in the responsiveness of specific genes and pathways that underlie color production, or both.

In *Sceloporus* and other lizards, blue abdominal coloration is produced through the organization of 2 distinct pigment cells. In the dermis, a layer of iridophores sits superficial to a layer of melanophores (Taylor and Hadley 1970; McLean et al. 2017; Nicolaï et al. 2021), the ectotherm homologs of mammalian melanocytes. The iridophores contain orderly stacks of guanine platelets that reflect different wavelengths of light depending upon their orientation, and the underlying melanophores produce melanin granules that absorb any light that is not reflected by the iridophores (Morrison et al. 1995). This cellular arrangement is exemplified by the blue skin of adult *S. undulatus* males, which results from both the reflection of blue light by iridophores and the absorption of other wavelengths by underlying melanophores (Fig. 1A–C). The presence of a similar iridophore layer in *S. undulatus* juveniles (C. D. Robinson, personal observation) and adult females (Fig. 1D–F), as well as in *S. virgatus* adults of either sex (Fig. 1G–L), suggests that elevated testosterone is not necessary for iridophore development, and that iridophores alone are insufficient for the expression of blue color. In *S. undulatus* and closely related *S. consobrinus* (previously *S. undulatus consobrinus*), as well as other phrynosomatid lizards in which males develop blue ventral coloration, testosterone stimulates melanin production in the dermis (Kimball and Erpino 1971; Quinn and Hews 2003; Cox et al. 2005, 2008). Consequently, the evolutionary loss of sexually dimorphic coloration in *S. virgatus* likely occurred primarily through the loss of melanin synthesis in ventral skin, rather than through changes in the iridophore layer (Fig. 2A and B). Therefore, we focus our a priori tests (see below) on genes and pathways that are involved in melanocortin production and melanin synthesis (Table 1 and Fig. 2C) as likely candidates for the evolutionary loss of responsiveness to androgen signaling. In addition to these specific downstream genes and pathways involved in melanin synthesis, we also focus on upstream pathways related to androgen metabolism, androgen availability, and androgen receptor expression (Table 1 and Fig. 2C).

To examine species differences in responsiveness to androgen signaling, we manipulated circulating testosterone levels in *S. undulatus* and *S. virgatus* juveniles and then used bulk RNAseq of ventral skin to compare gene expression between controls and individuals with experimentally elevated testosterone within each species. We conducted this experiment in juveniles to test for effects on gene expression prior to sexual divergence in circulating testosterone, which avoids any confounding effects of endogenous testosterone and allows us to assess the development of coloration prior to any natural induction by testosterone. We first characterized genes and pathways responsive to testosterone in *S. undulatus* to identify those that potentially contribute to the development of vibrant coloration in this sexually dimorphic species. We then explored which of these genes and pathways have different expression patterns or fail to respond to testosterone in *S. virgatus*, potentially explaining the loss of vibrant ventral color in this sexually monomorphic species. We approached this comparison using a combination of unbiased analyses across the entire skin transcriptome and targeted analyses of specific genes selected a priori to test several potential mechanisms for the evolutionary loss of hormonally mediated ventral coloration (Table 1 and Fig. 2C). Specifically, we tested whether these 2 closely related species differ in the expression of 1) upstream genes that mediate tissue sensitivity to androgens, 2) genes downstream from androgen signaling that regulate the production of melanin pigment, and 3) marker genes that indicate the presence of melanophores or melanophore precursors. Collectively, these analyses allow us to address an issue of general significance in evolutionary endocrinology (Cox et al. 2022): whether evolutionary changes in hormonally mediated phenotypes occur via upstream changes in tissue sensitivity to hormonal signals, downstream changes in hormonal responsiveness of target genes, or a combination of these mechanisms.

Methods

Experimental design and sample collection

We collected wild juvenile Eastern Fence Lizards (*S. undulatus*; sexually dichromatic) and Striped Plateau Lizards (*S. virgatus*; sexually monochromatic) at approximately 1

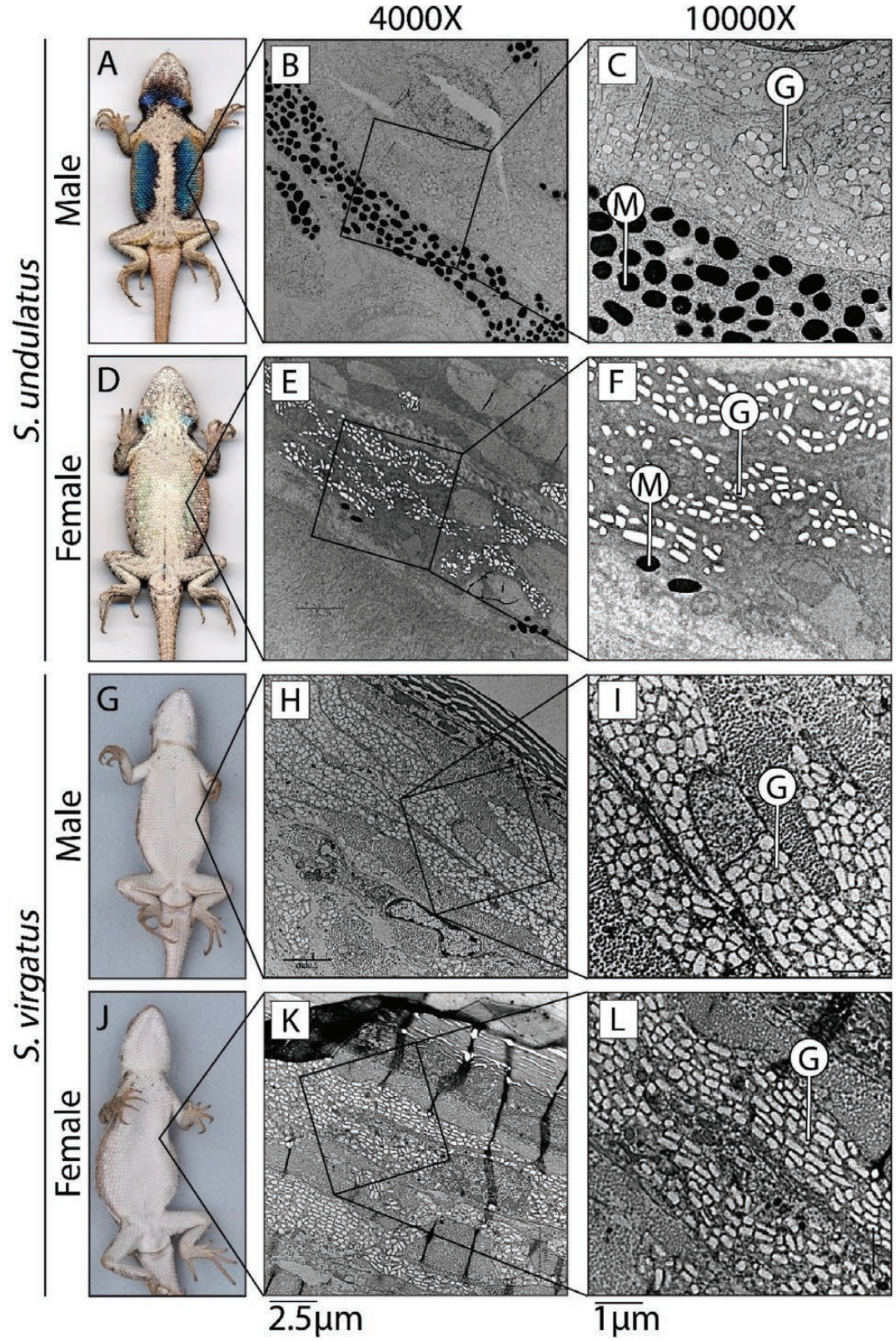

Fig. 1. Photographs and transmission electron micrographs of ventral skin in (A–C) *S. undulatus* males, (D–F) *S. undulatus* females, (G–I) *S. virgatus* males, and (J–L) *S. virgatus* females. Blue skin in *S. undulatus* males results from reflection of blue light by organized guanine platelets (G) within iridophores, and from absorption of other wavelengths by an underlying layer of melanin-filled melanosomes (M) within melanophores. Organized guanine platelets are present within iridophores of all 4 groups, but a pronounced melanophore layer of melanin-filled melanosomes is only present in *S. undulatus* males. Images from panels A and D were originally published in Cox et al. (2005a) by the American Society of Ichthyologists and Herpetologists. They are being used under a Creative Commons CC BY license.

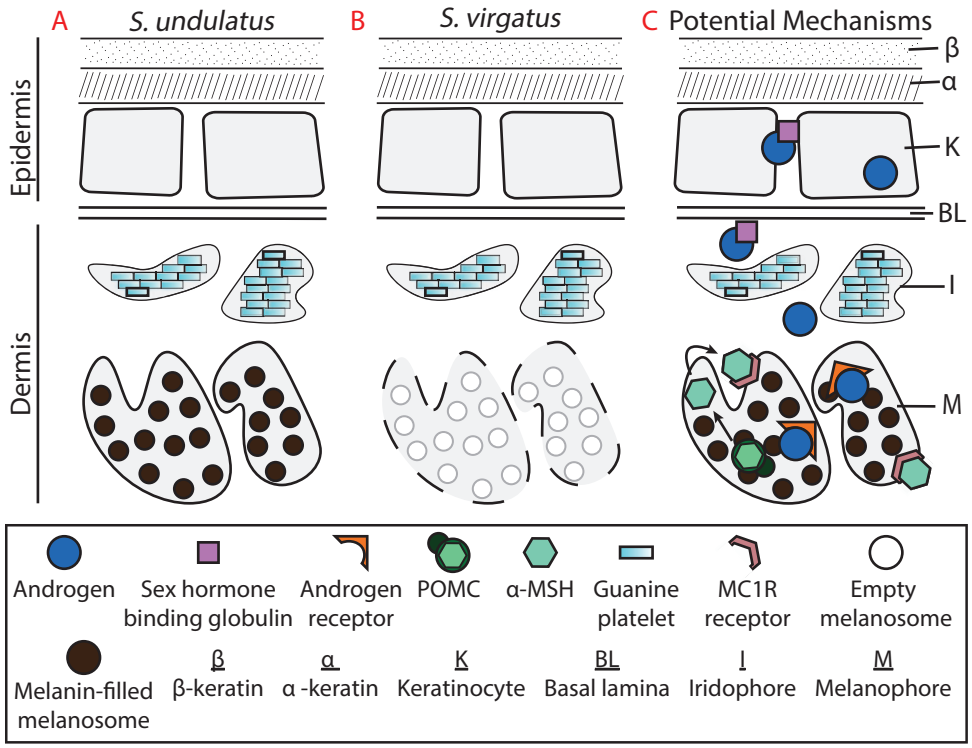

Fig. 2. Proposed model of ventral skin in (A) *S. undulatus* and (B) *S. virgatus*. Adult *S. undulatus* males have a layer of melanized melanophores deep to the iridophore layer, whereas *S. virgatus* males do not. Melanophores in *S. virgatus* are illustrated with dashed lines to indicate that it is unknown whether *S. virgatus* retains unpigmented melanophores in its ventral skin. (C) In *S. undulatus*, we hypothesize that free androgens bind the androgen receptor (AR) to induce melanin synthesis via production of proopiomelanocortin (POMC), which is processed into α-melanocyte stimulating hormone (α-MSH) that binds the melanocortin-1 receptor (MC1R) on the surface of melanophores to stimulate melanin synthesis.

mo of age and transported them to the University of Virginia, where they were housed individually in small terraria. After a 1-mo acclimation period, we split individuals of each species and sex into 2 size-matched treatment groups: one receiving a small intraperitoneal implant filled with 100 µg crystalline testosterone and one receiving an empty implant as a control. Implant construction and surgical procedures followed previous studies (Cox et al. 2015, 2017; Wittman et al. 2021) and were designed to elevate circulating testosterone to levels typical of breeding adult males of each species (Cox and John-Alder 2005; Cox et al. 2005a; John-Alder et al. 2009; Hews et al. 2012). Further details about sample collection, animal care, environmental conditions in captivity, methods for implant design, and protocols for surgery are provided as Supplementary Materials. Eight weeks after treatment, we quantified color development by taking ventral photographs of each animal and using Fiji (ImageJ 1.52v) software (Schindelin et al. 2012) and R v4.2.1 (R Core Team 2022) to estimate hue, saturation, and brightness. Hue represents the dominant wavelength, saturation represents a metric of color purity, and brightness represents closeness to white. For further details about color quantification, see the Supplementary Materials. The following day, we euthanized each animal via decapitation and immediately collected blood to confirm treatment effects on circulating testosterone levels via radioimmunoassay (see Supplementary Materials). We also immediately collected ventral skin from areas in which colorful abdominal patches develop in adult *S. undulatus* males (abdominal patches are absent in *S. virgatus* and in unmanipulated *S. undulatus* juveniles) into RNAlater (ThermoFisher Scientific) on ice, then refrigerated them for 24 h at 4 °C and stored them at −80 °C until RNA extraction.

We extracted RNA from skin of 48 juvenile lizards ($n = 6$ per treatment, per sex, per species) using Illustra RNAspin Mini RNA Isolation Kit (GE Healthcare) following manufacturer specifications with minor modifications (see Supplementary Materials). RNA quality was assessed using a Nanodrop spectrophotometer (ThermoFisher Scientific, Waltham Massachusetts) and Agilent 2100 BioAnalyzer (RNA 600 Pico; Agilent Biotechnologies, Santa Clara, California). Library preparation and sequencing were carried out by the Georgia Genomics and Bioinformatics Core (University of Georgia, Athens, Georgia). Two libraries (one *S. undulatus* control male, one *S. virgatus* testosterone male) were not sequenced due to low RNA concentrations. cDNA libraries were prepared from total RNA (~500 ng per sample) using KAPA Biosystems (Wilmington, Massachusetts) RNA library preparation chemistry with poly(A) selection. Libraries were sequenced on an Illumina NextSeq 2000 (2 × 100 bp paired-end sequencing) using P3 high-output flow cells. We assessed read quality and trimmed reads using Fastp (Chen et al. 2018) with paired-end base correction, low complexity filtering, 3′ end tail quality trimming (average phred threshold = 20; window size = 5), and poly(g) and poly(x) trimming enabled. We also applied an overall minimum length filter of 36 bp and minimum phred score threshold of 25, then aligned reads to the *S. undulatus* genome (Westfall et al. 2021; GCA_019175285.1, SceUnd_v1.1) using subread-align (Liao et al. 2013), with *S. undulatus* transcripts used as an alignment guide (GCF_019175285.1). Following alignment, we assigned both uniquely mapped fragments and singleton

Table 1. Genes selected a priori to test hypotheses for species differences in "Tissue sensitivity to testosterone," "melanocortin production and signaling," "mediation of melanin synthesis," and "presence of melanophores. "Tissue sensitivity" includes genes with products that influence androgen metabolism, androgen availability, and androgen receptor availability. "Melanocortin production and signalling" includes genes with products that produce and detect α-melanocyte stimulating hormone. "Mediation of melanin synthesis" includes genes with products that influence melanin synthesis. "Presence of melanophores" includes genes commonly used as molecular markers of melanophores and their cellular precursors. Bolded gene names and predictions indicate instances in which we find statistical support for our predictions.

Hypothesis	Gene	Product and function	Prediction for expression
Tissue sensitivity to testosterone Conclusion: *Partial support*	*CYP19A1*	Aromatase—converts testosterone (T) to estradiol, which cannot bind AR	Higher in *S. virgatus*
	SRD5A1 ***SRD5A2*** *SRD5A3*	5α-Reductase—converts T to more potent androgen 5α-dihydrotestosterone (5α-DHT), which also binds AR	**Higher in *S. undulatus***
	SHBG	Sex hormone-binding globulin—binds T and prevents androgen signaling	**Higher in *S. virgatus***
	AR	Androgen receptor (AR)—mediates gene expression when bound by T or 5α-DHT	Higher in *S. undulatus*
Melanocortin production and signaling Conclusion: *Partial support*	***POMC***	Proopiomelanocortin (POMC)—precursor to adrenocorticotropic hormone (ACTH) and α-melanocyte stimulating hormone (α-MSH)	**Higher in *S. undulatus*** and/or **upregulated by T in *S. undulatus***
	PCSK1	Prohormone convertase 1 (PC1)—cleaves POMC into ACTH	Higher in *S. undulatus* and/or upregulated by T in *S. undulatus*
	PCSK1N	proSAAS—inhibits PC1	**Lower in *S. undulatus*** and/or downregulated by T in *S. undulatus*
	PCSK2	Prohormone convertase 2—cleaves ACTH into α-MSH	Higher in *S. undulatus* and/or **upregulated by T in *S. undulatus***
	MC1R	Melanocortin-1 receptor—binds ACTH and α-MSH to regulate melanin synthesis	**Higher in *S. undulatus*** and/or upregulated by T in *S. undulatus*
Mediation of melanin synthesis Conclusion: *Strong support*	***TYR***	Tyrosinase—converts tyrosine into melanin precursors	**Higher in *S. undulatus*** and/or **upregulated by T in *S. undulatus***
	TYRP1	Tyrosinase-related protein 1—stabilizes tyrosinase in melanosomal membranes	**Higher in *S. undulatus*** and/or **upregulated by T in *S. undulatus***
	OCA2	P protein—regulates melanosome pH to facilitate melanin synthesis	Higher in *S. undulatus* and/or **upregulated by T in *S. undulatus***
Presence of melanophores Conclusion: *No support*	*DCT*	Dopachrome tautomerase—regulates melanophore survival	Not expressed in *S. virgatus*
	KIT	KIT protein—facilitates signaling to regulate cellular processes in melanophores	Not expressed in *S. virgatus*
	MITF	Microphthalmia-associated transcription factor—regulates melanophore processes	Not expressed in *S. virgatus*

reads to annotated *S. undulatus* genes using featureCounts (Liao et al. 2014) to generate a matrix of read counts.

Identification and functional characterization of testosterone-responsive genes

All statistical analyses were run in R v4.2.1 (R Core Team 2022). To characterize transcriptome-wide responses to testosterone in each species and identify testosterone-responsive genes with an unbiased approach, we conducted differential gene expression analysis on read counts from both species using the package edgeR v3.30.3 (Robinson et al. 2010). Prior to analysis, 2 libraries were removed due to low read counts (316k reads for a *S. undulatus* control female and 4.3 M reads for a *S. virgatus* control male). We removed genes with low expression using *filterByExpr* in edgeR, which retained 18,017 genes. We then conducted principal components analysis using *robpca* within rospca v1.0.4 (Reynkens 2018) to test for outlier libraries. Three *S. virgatus* libraries (one control female, one testosterone female, and one control male) were subsequently removed. In total, 41 libraries were included in differential expression analyses, with n = 4 to 6 libraries per treatment, per sex, per species (Table 2) and an average library size of 19.9 M reads in *S. undulatus* and 19.5 M reads in *S. virgatus*. We normalized read counts using trimmed mean of *M*-values (TMM) normalization and used *glmQLFit* in edgeR to fit a negative binomial model to our data, specifying robust = TRUE to reduce the influence of hypervariable genes (see Phipson et al. 2016). Finally, we used the function *glmQLFTest* to calculate quasi-likelihood *F*-tests for paired contrasts between treatment groups (testosterone vs. control) within each species, retaining the effect of sex in each species comparison. We conducted these same analyses without the effect of sex, and results were largely similar. We chose to present results from analyses including sex because an additional 787 genes pass filtering with this added biological information. Genes were considered significantly differentially expressed genes (hereafter, DEGs) if their *P*-value was less than 0.05 following Benjamini–Hochberg correction for false discovery (Benjamini and Hochberg 1995).

Table 2. Sample sizes for each species, sex, and treatment group. We extracted RNA from skin from 6 individuals per treatment, per sex, per species (48 total). Values here represent the numbers used in analysis after libraries were removed due to low RNA concentrations, low read counts, and visual examination of robustPCA plots.

Species	Control			Testosterone		
	Female	Male	Total	Female	Male	Total
S. undulatus	5	5	10	6	6	12
S. virgatus	5	4	9	5	5	10

To infer functions of genes that were differentially expressed in response to testosterone, we used gene ontology (GO) analysis (Ashburner et al. 2000; The Gene Ontology Consortium 2021). Specifically, we used the PANTHER Overrepresentation Test (PANTHER17.0; GO Ontology database DOI: 10.5281/zenodo.6799722) with Fisher's exact test to examine GO biological processes and cellular components. We tested for enrichment of biological processes with DEGs using all protein-coding genes from 3 species: *Homo sapiens* (human) as the default GO reference species; *Anolis carolinensis* (green anole) as a comparison to another lizard; and *Danio rerio* (zebrafish) as a comparison to a model organism for pigment cell development (Parichy 2021). Green anoles and zebrafish both have dermal iridophores, which are absent in mammals, so including these species facilitates the identification of biological processes and cellular components related to iridophore development that would not be detectable using only the default human database. We used these GO analyses to characterize genes and pathways that respond to testosterone in *S. undulatus* and identify those likely to underlie the development of ventral coloration in this sexually dimorphic species. We predicted that any pathways related to color that were enriched for DEGs in *S. undulatus* would not be enriched for DEGs in sexually monomorphic *S. virgatus*, in which testosterone does not induce vibrant ventral color.

Species differences in transcriptome-wide responsiveness to testosterone

To explore whether the loss of color in *S. virgatus* reflects a tissue-wide loss of transcriptomic responsiveness to testosterone, we first tested whether the total number of DEGs differed between species using a chi-square test with one degree of freedom. Because of differences in our statistical power to identify DEGs due to species differences in sample size (22 *S. undulatus* libraries, 19 *S. virgatus* libraries), we extended this analysis by iteratively dropping 3 *S. undulatus* libraries and recalculating the number of DEGs 1,540 times, covering all possible combinations in which 3 out of 22 individuals could be removed to achieve equal sample sizes between species. For each iteration, we used a chi-square test to compare the total number of DEGs between species, then calculated the proportion of comparisons in which the number of DEGs differed ($P < 0.05$) between species.

To assess the overall similarity of transcriptomic responsiveness to testosterone between species, we asked whether DEGs that were significantly up- or downregulated by testosterone in one species had $\log_2$-fold change ($\log_2$FC) values that were similarly different from zero in the other species. Specifically, we used Wilcoxon signed-rank tests to determine whether the median $\log_2$FC values of the DEGs upregulated by testosterone in one species were significantly greater than zero in the other species, and whether the median $\log_2$FC values of the DEGs downregulated by testosterone in one species were significantly less than zero in the other species. We conducted these analyses reciprocally using the sets of DEGs identified independently in each species. A significant *P*-value with the same fold-change direction would indicate that many of the genes that are responsive to testosterone in one species are similarly responsive to testosterone in the other species. When analyzing whether genes upregulated by testosterone in *S. undulatus* were upregulated in *S. virgatus*, we excluded any DEGs identified by GO analysis as residing within pigment-related biological pathways (Table 3) because we were interested specifically in testing whether other DEGs unrelated to melanin synthesis exhibited similar transcriptomic responses between species.

Species differences in expression of a priori candidate genes

To analyze effects of sex, species, and treatment on a gene-by-gene basis for the candidate genes that we selected a priori for their roles in tissue sensitivity to androgens, melanin synthesis, and melanophore differentiation (Table 1), we converted read counts to transcripts per million (TPM). We first conducted separate ANOVAs on each gene (17 total genes) by including effects of sex, species, and treatment, plus all pairwise and 3-way interactions. Because we were primarily interested in the effects of treatment and species, we conducted an additional analysis excluding sex and its interactions from the model. We then used the function *lrtest* from the lmtest package (Zeileis and Hothorn 2002) to test whether the full (including sex) or reduced (excluding sex) model best fit our data. We report results from the full model when the likelihood ratio test was significant and results from the reduced model when the likelihood ratio test was not significant. Consequently, sex and its interactions were only retained in analyses of expression for the genes *SRD5A3*, *POMC*, and *PCSK1N*.

Although we selected these genes a priori, we conservatively applied Bonferroni corrections to any *P*-values that could be viewed as multiple tests of the same mechanistic hypothesis (see below) when conducting these gene-specific analyses. Unadjusted *P*-values are reported unless results are no longer significant after Bonferroni correction, in which case the adjusted value (P_{adj}) is also reported. First, we used an adjusted critical value of $\alpha = 0.0083$ (6 tests) when assessing differences in the expression of 6 genes related to upstream androgen availability and/or tissue responsiveness to androgens. Second, we used an adjusted critical value of α

Table 3. Results from GO enrichment analysis testing for enriched pathways from genes upregulated by testosterone in *S. undulatus* juveniles. Analyses were conducted 3 times, examining over enrichment of protein-coding genes from 3 reference species (source of GO terms). Genes listed include all genes represented within nested processes for a term. Genes in bold are represented in more than one biological process. FDR is the *P*-value after correction for false discovery rate.

Source of GO terms	Biological process	Fold enrichment	Genes	FDR
Homo sapiens	Eye pigment biosynthetic process	>100	***EDN3, OCA2, PMEL, RAB27A, SLC45A2, TYR, TYRP1***	0.052
	Peptidoglycan transport	>100	*SLC15A2, SLC15A3*	0.045
	Melanin biosynthetic process	>100	***OCA2, PMEL, SLC45A2, TYR, TYRP1***	<0.001
	Melanocyte differentiation	80	***EDN3, OCA2, RAB27A, TYRP1***	<0.001
Anolis carolinensis	Melanin biosynthetic process	>100	***OCA2, TYR, TYRP1***	0.002
	Melanocyte differentiation	>100	***OCA2, PMEL, RAB27A, TYR,*** **TYRP1**	0.005
	Cellular pigmentation	86	***PMEL, RAB27A, TYRP1***	0.014
Danio rerio	Melanin biosynthetic process	>100	***OCA2, TYR***	0.001
	Melanocyte differentiation	93	***OCA2, SLC45A2, TYR***	<0.001

= 0.01 (5 tests) when assessing differences in the expression of 5 genes related melanocortin production and signaling. Third, we used an adjusted critical value of α = 0.016 (3 tests) when assessing differences in the expression of 3 genes related to melanin synthesis and when assessing differences in the expression of 3 other genes used as molecular markers for melanophores.

We selected 6 genes to test for species differences in upstream androgen metabolism, androgen availability, and tissue sensitivity to androgens (Table 1 and Fig. 2C). First, because testosterone can be locally converted to either estradiol (which does not activate the androgen receptor) or the more potent androgen 5α-dihydrotestosterone (DHT), we analyzed the expression of genes encoding aromatase (*CYP19A1*) and 5α-reductase (*SRD5A1*, *SRD5A2*, and *SRD5A3*), the enzymes that respectively mediate these steps in steroid metabolism. Second, because androgen signaling cannot be initiated when steroids are bound by globulins, we analyzed the expression of the gene encoding sex hormone-binding globulin (*SHBG*). Third, we assessed tissue sensitivity by analyzing the expression of the gene encoding androgen receptor (*AR*), which mediates the genomic effects of androgens on downstream genes. Analogous tests for the genes encoding estrogen receptor-α (*ESR1*) and estrogen receptor-β (*ESR2*) are reported in the Supplementary Materials. If changes to the regulation of any of these genes contribute to the evolutionary loss of color, we predicted that *S. virgatus* would exhibit 1) higher *CYP19A1* expression, 2) lower *SRD5A1-3* expression, 3) higher *SHBG* expression, and 4) lower *AR* expression, relative to *S. undulatus* (Table 1).

Next, we tested for species differences in hormonal responsiveness of key color genes downstream from androgen signaling. First, we tested for differences in 5 genes whose products contribute to the production, regulation, and detection of α-melanocyte stimulating hormone (α-MSH). Specifically, we examined expression patterns of the proopiomelanocortin gene (*POMC*) and genes encoding enzymes that contribute to the conversion of POMC to α-MSH (*PCSK1*, *PCSK2*, and *PCSK1N*). While *POMC* is expressed primarily in the pituitary, it can also be locally produced by keratinocytes and melanocytes in the skin (Schauer et al. 1994; Chakraborty et al. 1996; Wintzen et al. 1996; Rousseau et al. 2007). POMC is cleaved into its peptide derivatives adrenocorticotropic hormone (ACTH) and α-MSH by prohormone convertases 1 (*PCSK1*) and 2 (*PCSK2*), respectively (reviewed in Harno et al. 2018). Because α-MSH then binds to the melanocortin-1 receptor (MC1R) on the surface of melanophores to stimulate melanin synthesis, we also tested for differences in expression of *MC1R*, which encodes the MC1R receptor. Next, we tested for differences in the expression of 3 downstream genes involved in melanin synthesis within melanophores (*TYR*, *TYRP1*, and *OCA2*). The products of these genes play critical roles in converting tyrosine into melanin precursors (TYR; Raper 1928), stabilizing tyrosinase in the melanosomal membrane and contributing to melanosome biosynthesis (TYRP1; Boissy et al. 1996; Kobayashi et al. 1998), and regulating pH within the melanosome at optimal levels for melanin synthesis (the P protein, encoded by *OCA2*; Bellono et al. 2014). For most of these genes, we predicted that expression would be higher in *S. undulatus* than in *S. virgatus* and/or that testosterone would upregulate expression in *S. undulatus*, but not in *S. virgatus* (Table 1). However, because *PCSK1N* encodes an inhibitor of prohormone convertase 1 (Fricker et al. 2000; Qian et al. 2000), we predicted that expression would be lower in *S. undulatus* than in *S. virgatus* and/or that testosterone would downregulate expression in *S. undulatus*, but not in *S. virgatus* (Table 1).

Finally, we tested for expression of 3 genes used as molecular markers of melanophores: *DCT*, *KIT*, and *MITF*. In the context of melanophores, *DCT*, encoding dopachrome tautomerase, contributes to the regulation of melanophore survival, *KIT*, encoding a tyrosine kinase called the KIT protein, facilitates signaling that regulates cellular processes, and MITF, encoding microphthalmia-associated transcription factor, regulates melanophore processes. If these genes are not expressed in the skin of *S. virgatus*, this might suggest that any observed differences between these 2 species are due to the loss of this cell type in the ventral dermis. However, expression of these 3 genes would suggest that the cell type necessary for melanin synthesis is present, but does not attain a fully melanized state in *S. virgatus*. If the evolutionary loss of color is due to a loss of melanophore development in the skin, we would expect reduced or undetectable expression of these 3 genes in *S. virgatus*, relative to *S. undulatus* (Table 1).

Results

Confirming treatment effects on circulating testosterone and coloration

Our implants consistently elevated plasma testosterone concentrations measured at the end of the 8-wk experiment, regardless of species or sex (Fig. 3). For *S. undulatus*, there was a significant increase in circulating testosterone in the treatment group ($F_{1,16}$ = 74.23, P < 0.0001), with no sex effect ($F_{1,16}$ = 0.31, P = 0.589) or treatment × sex interaction ($F_{1,16}$ = 0.15, P = 0.705). Similarly, for *S. virgatus*, there was a significant increase in testosterone in the treatment group ($F_{1,15}$ = 75.51, P < 0.0001), with no sex effect ($F_{1,15}$ = 1.19, P = 0.293) or treatment × sex interaction ($F_{1,15}$ = 0.27, P = 0.614). In an omnibus model including sex, species, treatment, and all 2- and 3-way interactions, only treatment was significant ($F_{1,31}$ = 149.87, P < 0.0001; all other P > 0.44).

In the sexually dichromatic *S. undulatus*, testosterone treatment significantly decreased brightness (closeness to white; $F_{1,18}$ = 34.60, P < 0.001; Fig. 4A) and decreased hue (dominant wavelength; $F_{1,18}$ = 4.875, P = 0.041; Fig. 4B), yet had no effect on saturation (color purity; $F_{1,18}$ = 2.73, P = 0.116; Fig. 4C) of the lateral areas of ventral skin where patches develop. There were no sex effects or treatment × sex interactions for any aspect of skin coloration (all P > 0.14). In the sexually monochromatic *S. virgatus*, there were no treatment effects, sex effects, or treatment × sex interactions for any aspect of coloration (all P > 0.17; Fig. 4D–F). Lateral areas of melanized skin with faint blue color were evident on the abdomens of most *S. undulatus* juveniles that received testosterone implants, whereas the abdomens of all other groups were essentially white with little evidence of ventral patch formation (Supplementary Fig. S1).

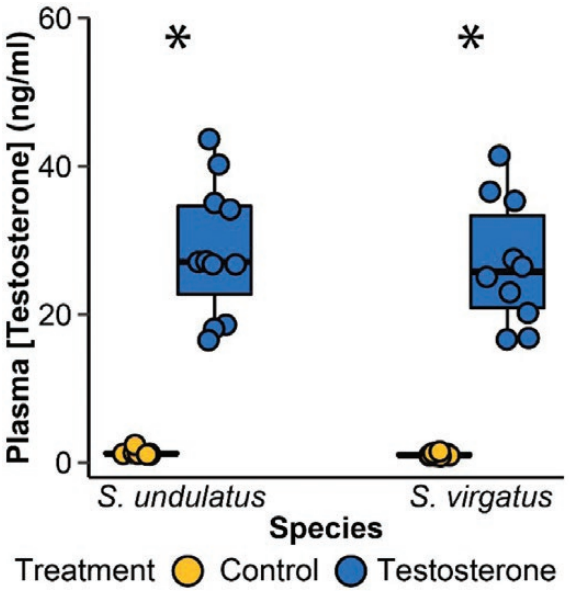

Fig. 3. Circulating levels of plasma testosterone for *S. undulatus* and *S. virgatus* at the time of tissue collection, 8 wk after implantation. Each circle is an individual, with boxplots illustrating the median (horizontal line), first and third quartiles (box), and 1.5 times the intraquartile range (whiskers) for each treatment group. Hormone implants significantly raised (P < 0.05, asterisks) circulating testosterone to similar levels in both species.

Identification and functional characterization of testosterone-responsive genes

In *S. undulatus*, the species in which maturing males develop vibrant blue and black ventral coloration, 278 genes were differentially expressed in the skin in response to testosterone (Fig. 5A), with 74 upregulated by testosterone (Supplementary Table S1) and 204 downregulated by testosterone (Supplementary Table S2). For *S. virgatus*, the species in which neither sex develops blue or black ventral coloration, only 55 genes were differentially expressed in the skin (Fig. 5B), with 30 upregulated by testosterone (Supplementary Table S3) and 25 downregulated by testosterone (Supplementary Table S4). Among the 74 genes that were significantly upregulated by testosterone in *S. undulatus*, GO enrichment revealed that pathways related to the melanin biosynthetic process and melanocyte (i.e. melanophore) differentiation were significantly enriched. Among the 5 total biological processes enriched across *H. sapiens*, *D. rerio*, and *A. carolinensis*, these 2 were the only shared processes across all 3 reference species (Table 3). Additionally, all but one of the other enriched processes (peptidoglycan transport) were related to pigmentation (Table 3). Among the 204 genes downregulated by testosterone in *S. undulatus*, enriched pathways included spermine biosynthesis process, mitotic spindle midzone assembly, and positive regulation of ubiquitin protein ligase activity, among others (Supplementary Table S5). There were no enriched pathways in *S. virgatus*.

Species differences in transcriptome-wide responsiveness to testosterone

The number of testosterone-responsive DEGs in the sexually dichromatic *S. undulatus* was significantly greater than in the sexually monochromatic *S. virgatus* whether we compared all DEGs (278 vs. 55 genes; χ^2 = 161.88, P < 0.001) or the subsets that were upregulated (74 vs. 30; χ^2 = 18.615, P < 0.001) or downregulated (204 vs. 25; χ^2 = 139.92, P < 0.001) by testosterone (Fig. 5A and B). When we iteratively excluded every possible combination of 3 *S. undulatus* libraries to ensure equal statistical power in each species, we found that the number of DEGs was significantly (P < 0.05) higher in *S. undulatus* than in *S. virgatus* for 1,487 of 1,540 iterations (96.6%), and that the mean (± 1 SD) number of DEGs was 3.71 ± 1.93 times greater in *S. undulatus* ($\bar{x} = 153.7 \pm 96.1$) than in *S. virgatus* ($\bar{x} = 40.4 \pm 8.3$). There were no cases in which *S. virgatus* had significantly more DEGs than *S. undulatus*. Therefore, species differences in transcriptome-wide responsiveness to testosterone are robust to the minor difference in sample size between species (Supplementary Fig. S2).

Seven of the genes that were significantly upregulated by testosterone in the sexually dichromatic *S. undulatus* are related to pigmentation and melanin synthesis pathways (Table 3), and these 7 genes were completely unresponsive to testosterone in the sexually monochromatic *S. virgatus* (Fig. 5A and B, red symbols). When excluding these 7 genes, the remaining 67 genes that were significantly upregulated by testosterone in *S. undulatus* had $\log_2$FC values that were significantly greater than zero in *S. virgatus* (V = 1442, P = 0.016; Fig. 5C). Likewise, genes that were significantly downregulated by testosterone in *S. undulatus* had $\log_2$FC values that were significantly less than zero in *S. virgatus* (V = 7276, P < 0.001;

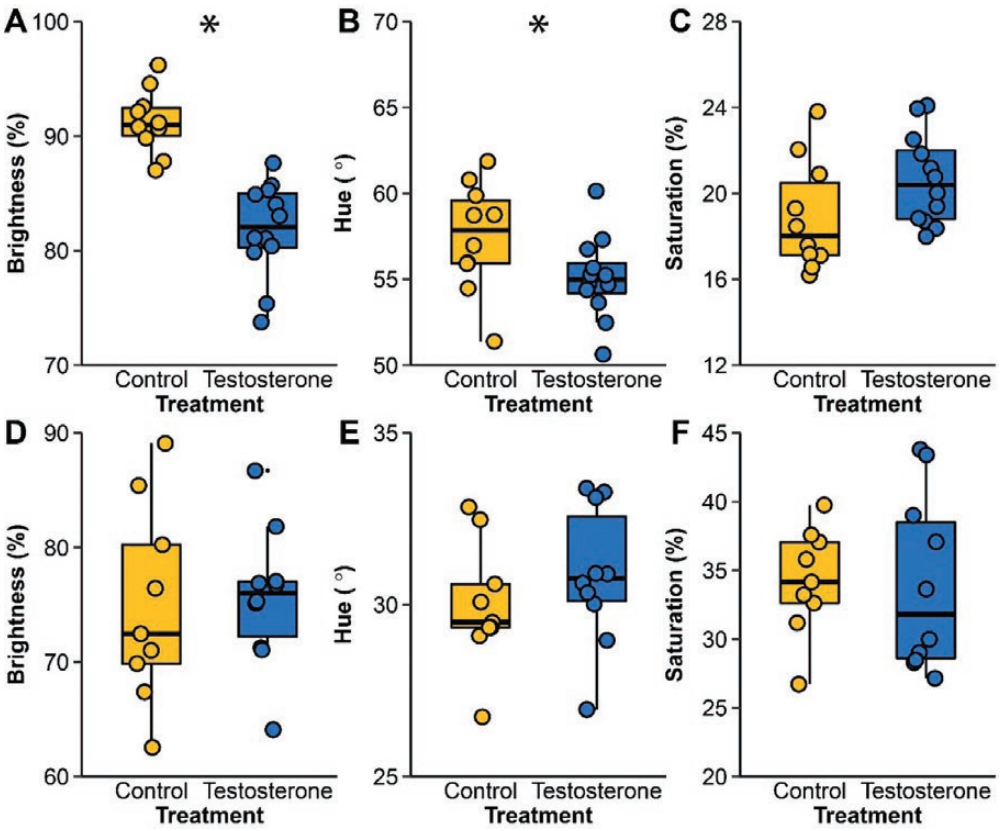

Fig. 4. Effects of testosterone on 3 aspects of ventral color in (A–C) *S. undulatus* and (D–F) *S. virgatus*. Each circle is an individual, with boxplots illustrating the median (horizontal line), first and third quartiles (box), and 1.5 time the intraquartile range (whiskers) for each treatment group. Testosterone decreased brightness and hue ($P < 0.05$, asterisks) in *S. undulatus*, but had no effect on coloration in *S. virgatus*.

Fig. 5C). Reciprocally, genes that were significantly up- or downregulated by testosterone in *S. virgatus* also displayed similar patterns of upregulation ($V = 388$, $P < 0.001$; Fig. 5C) or downregulation ($V = 59$, $P = 0.004$; Fig. 5C) in *S. undulatus*. A total of 95 genes were upregulated by testosterone in either species, with 9 genes significantly upregulated by testosterone in both species (Fig. 5D). A total of 225 genes were downregulated by testosterone in either species, with 4 of these genes were significantly downregulated by testosterone in both species (Fig. 5D). While the overall trend was for genes to respond similarly to testosterone in both species (Fig. 5C), many genes were responsive in one species yet unresponsive in the other (Fig. 5C and D).

Species differences in genes mediating androgen availability and tissue sensitivity

SRD5A2, one of the 3 genes encoding the 5α-reductase enzyme that converts testosterone to the more potent androgen 5α-DHT, was expressed at higher levels in the sexually dichromatic *S. undulatus* than in the sexually monochromatic *S. virgatus* ($F_{1,37} = 17.11$, $P < 0.001$), was downregulated by testosterone ($F_{1,37} = 24.75$, $P < 0.001$), and had no treatment × species interaction ($F_{1,37} = 1.29$, $P = 0.263$; Fig. 6B). Neither *SRD5A1* nor *SRD5A3* exhibited a significant treatment effect, species effect, or treatment × species interaction (all $P > 0.089$), although males exhibited higher expression of *SRD5A3* than females ($F_{1,33} = 9.34$, $P = 0.004$). *CYP19A1*, which encodes the aromatase enzyme that converts testosterone to estradiol, was not expressed at detectable levels in the skin of either species. *SHBG*, which encodes sex hormone-binding globulin, was expressed at higher levels in *S. virgatus* than in *S. undulatus* ($F_{1,37} = 20.72$, $P < 0.001$), with no effect of testosterone ($F_{1,37} = 0.86$, $P = 0.359$) or treatment × species interaction ($F_{1,37} = 0.07$, $P_{adj} = 1$; Fig. 6A). *AR*, which encodes the androgen receptor, was expressed at higher levels in *S. virgatus* than in *S. undulatus* ($F_{1,37} = 14.65$, $P < 0.001$) and was downregulated by testosterone ($F_{1,37} = 10.86$, $P = 0.002$) similarly in both species (treatment × species interaction: $F_{1,37} = 1.44$, $P = 0.238$; Fig. 6C).

Species differences in genes mediating melanocortin production and signaling

Our expression data collectively suggest that the production of POMC and its conversion to α-MSH are both stimulated by testosterone in the sexually dichromatic *S. undulatus*, but not in the sexually monochromatic *S. virgatus*, and that the α-MSH signal is more likely to be detected in *S. undulatus* due to relatively higher expression of the gene for its MC1R receptor. *POMC*, which encodes proopiomelanocortin, was expressed at much higher levels in *S. undulatus* than in *S. virgatus*, in which its expression was barely detectable in control animals ($F_{1,33} = 43.15$, $P < 0.001$). *POMC* expression was significantly increased by testosterone ($F_{1,33} = 7.92$, $P = 0.008$) in both species (treatment × species interaction: $F_{1,33} = 3.60$, $P = 0.066$), although its expression was much lower in *S. virgatus* than in *S. undulatus* even in the presence of exogenous testosterone (Fig. 6D). *PCSK1*, which encodes the enzyme that converts POMC to adrenocorticotrophic hormone

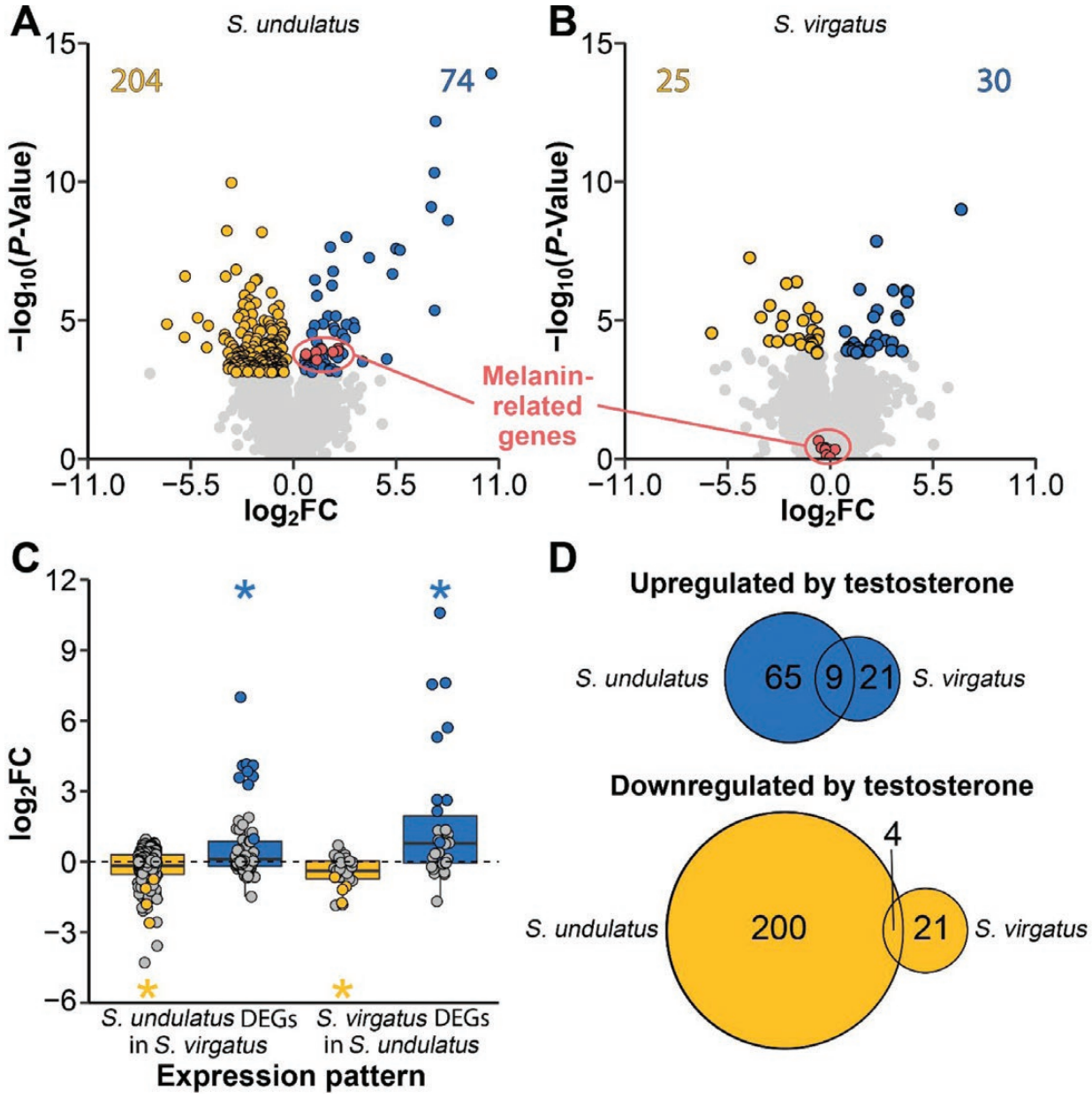

Fig. 5. Volcano plots of the $-\log_{10}$ *P*-value for the effect of testosterone on expression against the $\log_2$-fold change (FC) between testosterone and control groups for 18,017 genes (circles) in (A) *S. undulatus* and (B) *S. virgatus*. Positive values represent genes upregulated by testosterone while negative values represent genes downregulated by testosterone. Colored symbols and numbers at the top of each panel indicate genes that are significantly differentially expressed between treatment groups after Benjamini–Hochberg correction. Red symbols represent melanin-related genes identified from GO analyses (Table 3). Gray symbols indicate genes that are not differentially expressed. (C) Distributions of $\log_2$FC values in the opposite species for the DEGs from panels A and B, with individual genes plotted as circles and boxplots reporting the median (horizontal line), first and third quartiles (box), and 1.5 times the interquartile range (whiskers) of values in each category. Blue boxplots represent genes that were upregulated by testosterone in panels A and B, while yellow boxplots represent genes that were downregulated by testosterone. Colored symbols represent genes that were differentially expressed in both species. Asterisks denote distributions that differ significantly from zero, indicating that effects of testosterone on expression are similar across species. (D) Venn diagrams illustrating the number of shared and unique DEGs up- or downregulated by testosterone between *S. undulatus* and *S. virgatus*.

(ACTH), was expressed at higher levels in *S. virgatus* than in *S. undulatus* ($F_{1,37}$ = 9.44, P = 0.004), but exhibited no treatment effect ($F_{1,37}$ = 0.51, P = 0.482) or treatment × species interaction ($F_{1,37}$ = 0.94, P = 0.338). *PCSK2*, which encodes the enzyme that subsequently converts ACTH to α-MSH, did not differ in expression by species ($F_{1,37}$ = 0.57, P = 0.454) or treatment ($F_{1,37}$ = 2.68, P = 0.110), but had a significant treatment × species interaction ($F_{1,37}$ = 8.59, P = 0.006; Fig. 6E), such that testosterone increased *PCSK2* expression in *S. undulatus* but not in *S. virgatus*. *PCSK1N*, which encodes proSAAS, an inhibitor of the conversion of POMC to ACTH, was expressed at higher levels in *S. virgatus* than in *S. undulatus* ($F_{1,33}$ = 13.26, P < 0.001), but was only weakly affected by testosterone ($F_{1,33}$ = 5.60, P = 0.024, P_{adj} = 0.114) and exhibited no treatment × species interaction ($F_{1,33}$ = 2.06, P = 0.160). *MC1R*, which encodes the melanocortin-1

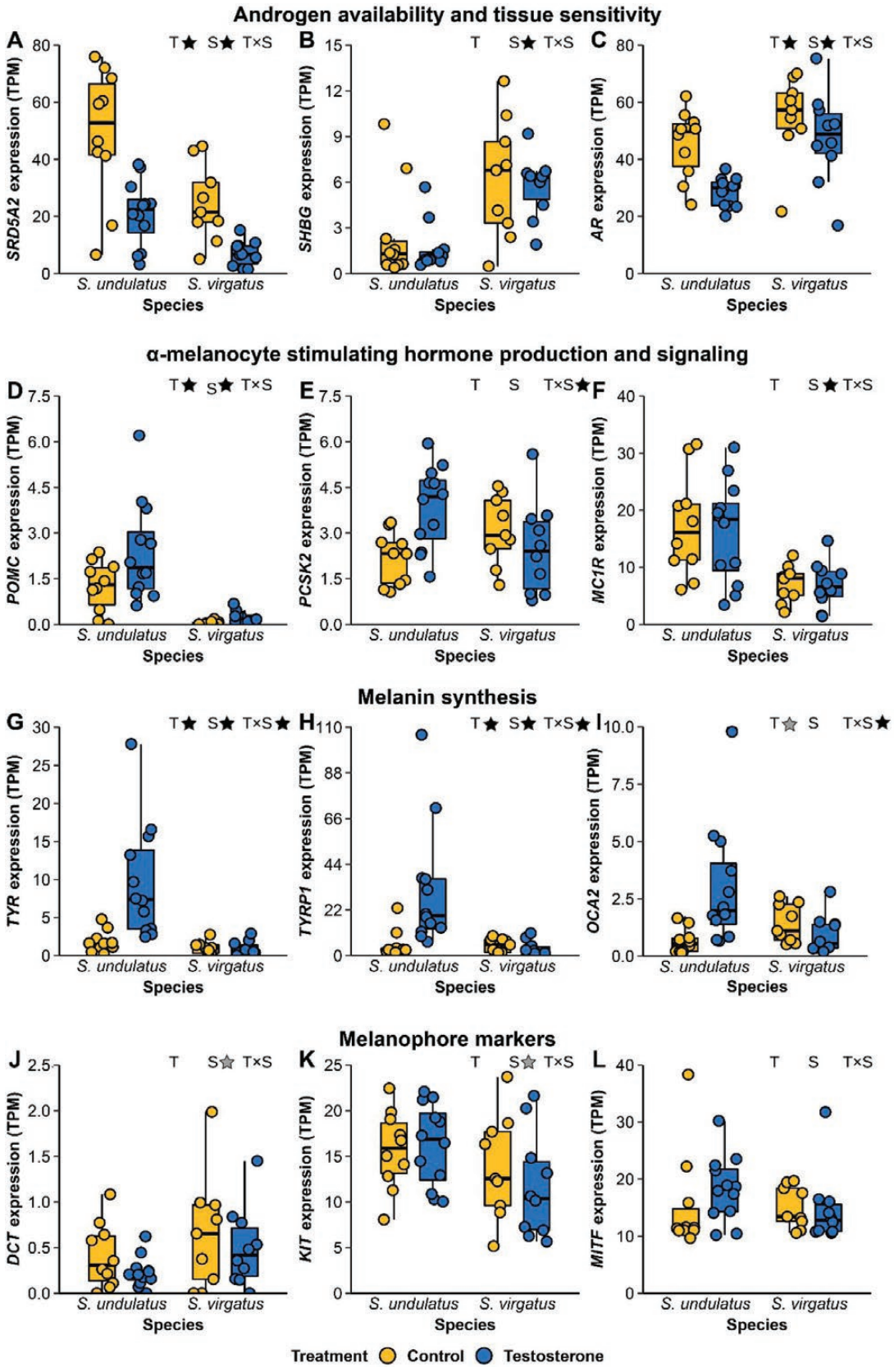

Fig. 6. Gene expression (TPM) as a function of species and testosterone treatment for 9 candidate genes selected a priori because of their roles mediating (A–C) androgen metabolism, availability, and signaling, (D–F) α–melanocyte stimulating hormone production, (G–I) production of melanin pigment, and (J–L) as molecular markers of melanophores at different stages of development. Boxplots illustrate the median (horizontal line), first and third quartiles (box edges) and 1.5 times the interquartile range (whiskers) for individual values (circles) in each group. Significant terms from ANOVA including hormone treatment (T), species (S), and treatment × species interactions (T × S) are represented by gray stars to the right of each model term when $P < 0.05$ and black stars to the right of each model term when $P_{adj} < 0.05$ (adjusting for multiple comparisons across several genes in a given mechanistic pathway).

receptor, was expressed at higher levels in *S. undulatus* than in *S. virgatus* ($F_{1,37}$ = 19.46, P < 0.001; Fig. 6F), with no treatment effect ($F_{1,37}$ = 0.04, P = 0.846) or treatment × species interaction ($F_{1,37}$ = 0.04, P = 0.840).

Species differences in genes mediating melanin synthesis

Our expression data collectively suggest that melanin synthesis is stimulated at the transcriptional level by testosterone in the sexually dichromatic *S. undulatus*, but not in the sexually monochromatic *S. virgatus*. *TYR*, which encodes tyrosinase, was expressed at higher levels in *S. undulatus* than in *S. virgatus* ($F_{1,37}$ = 14.73, P < 0.001), upregulated by testosterone ($F_{1,37}$ = 10.24, P = 0.003), and upregulated more strongly in *S. undulatus* than in *S. virgatus* (treatment × species interaction: $F_{1,37}$ = 8.80, P = 0.005; Fig. 6G). We observed similar patterns for *TYRP1*, which encodes tyrosinase-related protein 1, such that it was expressed higher in *S. undulatus* ($F_{1,37}$ = 8.54, P = 0.006), upregulated by testosterone ($F_{1,37}$ = 6.88, P = 0.013), and upregulated more strongly in *S. undulatus* than in *S. virgatus* (treatment × species interaction: $F_{1,37}$ = 6.85, P = 0.013; Fig. 6H). *OCA2*, which encodes the P protein, exhibited a significant treatment × species interaction ($F_{1,37}$ = 8.28, P = 0.007; Fig. 6I), but no significant species ($F_{1,37}$ = 2.32, P = 0.137) or treatment ($F_{1,37}$ = 4.61, P_{adj} = 0.111, P = 0.038) effects.

Expression of marker genes for melanophores and their precursors

Genes selected as markers for melanophores or melanophore precursors were expressed in both species and were unresponsive to testosterone in either species. *DCT*, which encodes dopachrome tautomerase, was expressed similarly in both species ($F_{1,37}$ = 4.14, P = 0.049, P_{adj} = 0.127), with no treatment effect ($F_{1,37}$ = 1.84, P = 0.183) or treatment × species interaction ($F_{1,37}$ = 0.01, P = 0.939; Fig. 6J). *KIT*, which encodes a tyrosine kinase called the KIT protein, was expressed similarly in both species ($F_{1,37}$ = 4.33, P = 0.044, P_{adj} = 0.127), with no treatment effect ($F_{1,37}$ = 0.17, P = 0.686) or treatment × species interaction ($F_{1,37}$ = 0.76, P = 0.388; Fig. 6K). *MITF*, which encodes the melanocyte-inducing transcription factor (also known as microphthalmia-associated transcription factor), was expressed similarly in both species ($F_{1,37}$ = 1.03, P = 0.318), with no treatment effect ($F_{1,37}$ = 0.51, P = 0.480) or treatment × species interaction ($F_{1,37}$ = 0.68, P = 0.415; Fig. 6L).

Discussion

We found that the evolutionary loss of hormonally mediated ventral coloration is associated with the loss of transcriptional responsiveness to testosterone by genes putatively involved in the production of ventral coloration. Whereas several key melanin synthesis genes were upregulated in response to testosterone in sexually dichromatic *S. undulatus*, these same genes were unresponsive to exogenous testosterone in sexually monochromatic *S. virgatus*. This does not appear to be due to the absence of melanophores in the skin of *S. virgatus*, given that we detected the expression of genes characteristic of melanophores at similar levels in the skin of both species. Nor does it appear to be because the ventral skin of *S. virgatus* is insensitive to androgens, given that we detected higher relative expression of the androgen receptor in *S. virgatus* and that transcriptome-wide patterns of up- and downregulation by testosterone were directionally similar in both species. However, we did find some evidence for lower transcriptional sensitivity to testosterone in the skin of *S. virgatus* than in *S. undulatus*. In particular, we found 3.7 times fewer genes that were differentially expressed in response to exogenous testosterone in *S. virgatus* relative to *S. undulatus*. We also found that *S. virgatus* skin expressed significantly less *SRD5A2*, which encodes the enzyme that converts testosterone into the more potent DHT, and significantly more *SHBG*, which encodes a binding globulin that prevents androgen signaling, relative to *S. undulatus*. Below, we discuss these mechanisms in greater detail and integrate them with recent theory and empirical work on the evolution of hormonally mediated sexual dimorphism.

The expression of genes that mediate melanin synthesis within melanophores (i.e. *TYR*, *TYRP1*, and *OCA*) was generally stimulated by testosterone in the sexually dichromatic *S. undulatus*, but was low and unresponsive to testosterone in the sexually monochromatic *S. virgatus*. These genes are critical for the production of melanin, and mutations in these genes are associated with atypical melanin-based phenotypes across taxa, including clinical abnormalities in humans (Yokoyama et al. 1990; Kelsh et al. 1996; Passmore et al. 1999; Toyofuku et al. 2001; King et al. 2003; Lyons et al. 2005a,b; Oetting et al. 2005; Klaassen et al. 2018; Li et al. 2019). However, coding sequence mutations typically result in systemic pigmentation effects rather than localized changes like those observed between *S. undulatus* and *S. virgatus*. In contrast, regulatory changes in gene expression can result in the evolution of morphology (Carroll 1995; Prud'homme et al. 2007; Wittkopp and Kalay 2012; Horton et al. 2014; Sackton et al. 2019; Merritt et al. 2020; Huang et al. 2022; Luecke et al. 2022), including phenotypes dependent upon melanin production (Gompel et al. 2005; Prud'homme et al. 2006; Werner et al. 2010; Koshikawa et al. 2015; Kratochwil et al. 2018; Koshikawa 2020; Hughes et al. 2023). Our results therefore suggest that the loss of ventral color in *S. virgatus* is at least partially due to the loss of androgen-dependent expression of these key melanin synthesis genes in the ventral skin. However, the mechanisms that underlie this loss of androgen responsiveness are less clear.

One hypothetical mechanism for the loss of androgen responsiveness by melanin synthesis genes is that mature melanophores are absent from the ventral skin of sexually monochromatic *S. virgatus*. The loss of this cell type may alter the transcriptomic profile of the skin and therefore explain both the low expression of individual melanin synthesis genes and the overall reduction in androgen responsiveness of the skin transcriptome in *S. virgatus*, relative to sexually dichromatic *S. undulatus*. However, contrary to this hypothesis, we detected expression of 3 melanophore-specific lineage markers at comparable levels in the skin of both species (*DCT*, *KIT*, and *MITF*; Steel et al. 1992; Parichy et al. 1999; Bondurand et al. 2000; Kelsh et al. 2000; Quigley et al. 2004; Mort et al. 2015; Schartl et al. 2016). This result suggests that melanophores or their melanoblast precursors are present in the skin of *S. virgatus*, although we cannot determine their developmental stage. The reduced expression of both *POMC* and *MC1R* in *S. virgatus*, relative to *S. undulatus*, could indicate that melanophores are in an immature state and

therefore unable to produce (POMC) and receive (MC1R) the necessary melanocortin signals to promote melanin synthesis. However, the location of POMC synthesis is unknown in our system and could occur in keratinocytes or melanophores (Schauer et al. 1994; Chakraborty et al. 1996; Wintzen et al. 1996; Rousseau et al. 2007), such that the use of *POMC* expression for inferences about melanophore development is tenuous. Nonetheless, our data indicate that melanophores are present in the skin of *S. virgatus*, but do not receive the necessary signals to mature or to initiate melanin production.

The reduced expression of *MC1R* that we observed in the skin of *S. virgatus* is one potential mechanism for the failure of melanophores to express melanin synthesis genes. Generally, MC1R binds α-MSH, which induces a cAMP cascade, resulting in increased expression of *MITF* and downstream melanin synthesis pathways (reviewed in Park et al. 2009). Therefore, the reduction in *MC1R* expression that we observed in *S. virgatus* could explain some of the observed species differences in the expression of *TYR*, *TYRP1*, and *OCA2*. Coding sequence mutations in *MC1R* have been shown to underlie whole-body color evolution in several vertebrates (Nachman et al. 2003; Rosenblum et al. 2004, 2010; Mundy 2005; Jin et al. 2020). Upstream from MC1R, reductions in the production and processing of POMC into α-MSH, which binds MC1R to initiate melanin synthesis, could also explain the low expression of *TYR*, *TYRP1*, and *OCA2* in *S. virgatus*. Our data support this possibility in that the expression of *POMC* is extremely low in *S. virgatus* relative to *S. undulatus*, and is stimulated by testosterone in *S. undulatus*, but not *S. virgatus*. Moreover, some genes whose products are involved in the processing of POMC into α-MSH are only responsive to androgens in *S. undulatus*. For example, *PCSK2* is upregulated by testosterone in *S. undulatus*, but it is not responsive to testosterone in *S. virgatus*. Therefore, the production of α-MSH in response to testosterone is likely greater in *S. undulatus*, increasing activation of the MC1R receptor and promoting melanin synthesis. Collectively, our data suggest that the loss of ventral coloration in *S. virgatus* occurs partly through the loss of *POMC* expression and processing in response to androgens, and partly through reductions in *MC1R* expression, resulting in the failure of testosterone to induce expression of melanin synthesis genes.

Finally, the question remains of whether and how overall sensitivity to androgens is reduced in the skin of the sexually monochromatic *S. virgatus*. Our data indicate that this is not due to the wholesale loss of androgen receptor expression in the skin, as *AR* was expressed robustly in both species, with slightly elevated expression in *S. virgatus*. However, we cannot eliminate the possibility of cell-specific changes in the expression of androgen receptor that are not captured by our bulk RNAseq approach. For example, *AR* could be expressed in *S. virgatus* keratinocytes and iridophores, but not in *S. virgatus* melanophores, preventing their maturation and subsequent melanization in response to androgen signaling (Schartl et al. 1982) while maintaining transcriptome-wide expression of *AR*. Rigorously addressing this possibility would require a more targeted approach, such as AR staining and localization via immunohistochemistry, in situ hybridization, or single-cell RNAseq. Support for this hypothesis would represent a case of a single-cell type within a tissue "unplugging" from hormonal control (Hau 2007; Ketterson et al. 2009). Although our data do not provide any evidence of reduced *AR* expression in *S. virgatus*, they do suggest that testosterone may be more readily converted to the more potent androgen 5α-DHT in *S. undulatus*, based on higher expression of *SRD5A2* (but not of *SRD5A1* or *SRD5A3*). Differences in the conversion of testosterone to 5α-DHT could lead to species-specific patterns of gene expression (Lin and Chang 1997; Dadras et al. 2001). Additionally, *SHBG* was expressed at higher levels in *S. virgatus* than in *S. undulatus*, potentially reducing the local availability of free androgens in the skin of *S. virgatus* (Anderson 1974; Breuner and Orchinik 2002).

The evolution of hormonally mediated sexual dimorphism proceeds not only through changes in circulating hormone levels (e.g. Husak and Lovern 2014), but also through changes in hormone–phenotype couplings (Cox 2020; Cox et al. 2022). For example, evolutionary changes in tissue-specific expression of the androgen receptor in manakins (Fuxjager et al. 2015) and anole lizards (Johnson et al. 2018) correspond to evolutionary changes in male-typical behaviors across species. Likewise, changes in the genomic distribution of hormone response elements may contribute to the evolution of sex-specific songs and display behaviors in birds (Frankl-Vilches et al. 2015; Fuxjager and Schuppe 2018) and sexual size dimorphism in primates (Anderson and Jones 2022). Having genomes for both *Sceloporus* species would permit similar comparisons of hormone response elements in this system, but currently there is no genome available for *S. virgatus*. We contribute to this emerging perspective in evolutionary endocrinology by showing that the evolution of sexually dimorphic coloration is associated with 1) pronounced changes in the hormonal responsiveness of downstream genes that mediate coloration, and 2) potential upstream changes in tissue sensitivity to a hormonal cue. Further exploration of these mechanisms will help clarify how phenotypes become evolutionarily decoupled from their hormonal regulators, facilitating the evolution of hormone–phenotype couplings and sexual dimorphism.

Supplementary material

Supplementary material is available at *Journal of Heredity* online.

Acknowledgments

All procedures involving animals were approved by the University of Virginia's Animal Care and Use Committee (protocol 3896). Animals were collected under permits from New Jersey Fish & Wildlife (SC 2019007), Arizona Game & Fish (SP658032), and the U.S. Forest Service (Coronado National Forest). This work used the JEOL 1230 Transmission Electron Microscope in the Advanced Microscopy Facility, which is supported by the University of Virginia School of Medicine. We thank S. Criswell for preparing tissues for imaging, C. Jeitner for assistance with radioimmunoassays, and the University of Georgia Genomics and Bioinformatics Core for library preparation and sequencing. Finally, we thank 2 anonymous reviewers for comments that improved this manuscript.

Funding

This work was supported by an Evolutionary, Ecological, or Conservation Genomics Research Award from the American Genetic Association (to C.D.R.); a Grants in Aid of Research

award from the Society for Integrative and Comparative Biology (to C.D.R.); a Graduate Student and Postdoc Association Research Award from University of Virginia (to C.D.R.); startup funding from Florida International University (to C.L.C.); USDA funding through McIntire-Stennis (NJ17321) and Hatch-Multistate (NJ17280) awards (to H.B.J.-A.); and a Collaborative Research award from the U.S. National Science Foundation (IOS 1755134 to C.L.C., IOS 1754934 to H.B.J.-A., and IOS 1755026 to R.M.C.).

Conflict of Interest

The authors declare no conflict of interest.

Data availability

Phenotypic data are available on Dryad at https://doi.org/10.5061/dryad.7d7wm381c. Reads from RNAseq are available under BioProject ID PRJNA1003887 at the National Center for Biotechnology Information Short Read Archive.

References

Abell AJ. Reproductive and post-reproductive hormone levels in the lizard *Sceloporus virgatus*. *Acta Zool Mex*. 1998a;74:43–57. doi:10.21829/azm.1998.74741720

Abell AJ. The effect of exogenous testosterone on growth and secondary sexual character development in juveniles of *Sceloporus virgatus*. *Herpetologica*. 1998b;54(4):533–543.

Anderson DC. Sex-hormone-binding globulin. *Clin Endocrinol (Oxf)*. 1974;3(1):69–96.

Anderson AP, Falk JJ. Cross-sexual transfer revisited. *Integr Comp Biol*. 2023:icad021. doi:10.1093/icb/icad021

Anderson AP, Jones AG. The relationship between sexual dimorphism and androgen response element proliferation in primate genomes. *Evolution*. 2022;76(6):1331–1346.

Anderson AP, Rose E, Flanagan SP, Jones AG. The estrogen-responsive transcriptome of female secondary sexual traits in the gulf pipefish. *J Hered*. 2020;111(3):294–306.

Ansai S, Mochida K, Fujimoto S, Mokodongan DF, Sumarto BKA, Masengi KWA, Hadiaty RK, Nagano AJ, Toyoda A, Naruse K, et al. Genome editing reveals fitness effects of a gene for sexual dichromatism in Sulawesian fishes. *Nat Commun*. 2021;12(1):1350.

Ashburner M, Ball CA, Blake JA, Botstein D, Butler H, Cherry JM, Davis AP, Dolinski K, Dwight SS, Eppig JT, et al. Gene ontology: tool for the unification of biology. *Nat Genet*. 2000;25(1):25–29.

Bellono NW, Escobar IE, Lefkovith AJ, Marks MS, Oancea E. An intracellular anion channel critical for pigmentation. *eLife*. 2014;3:e04543. doi:10.7554/eLife.04543

Benjamini Y, Hochberg Y. Controlling the false discovery rate: a practical and powerful approach to multiple testing. *J R Stat Soc*. 1995;57(1):289–300.

Blázquez MA, Nelson DC, Wijers D. Evolution of plant hormone response pathways. *Annu Rev Plant Biol*. 2020;71(1):327–353.

Boissy RE, Zhao H, Oetting WS, Austin LM, Wildenberg SC, Boissy YL, Zhao Y, Sturm RA, Hearing VJ, King RA, et al. Mutation in and lack of expression of tyrosinase-related protein-1 (TRP-1) in melanocytes from an individual with brown oculocutaneous albinism: a new subtype of albinism classified as "OCA3". *Am J Hum Genet*. 1996;58(6):1145–1156.

Bondurand N, Pingault V, Goerich DE, Lemort N, Sock E, Le Caignec C, Wegner M, Goossens M. Interaction among *SOX10*, *PAX3*, and *MITF*, three genes altered in Waardenburg syndrome. *Hum Mol Genet*. 2000;9(13):1907–1917.

Breuner CW, Orchinik M. Plasma binding proteins as mediators of corticosteroid action in vertebrates. *J Endocrinol*. 2002;175(1):99–112.

Carroll SB. Homeotic genes and the evolution of arthropods and chordates. *Nature*. 1995;376(6540):479–485.

Chakraborty AK, Funasaka Y, Slominski A, Ermak G, Hwang J, Pawelek JM, Ichihashi M. Production and release of proopiomelanocortin (POMC) derived peptides by human melanocytes and keratinocytes in culture: regulation by ultraviolet B. *Biochem Biophys Acta*. 1996;1313(2):130–138.

Chen S, Zhou Y, Chen Y, Gu J. fastp: an ultra-fast all-in-one FASTQ preprocessor. *Bioinformatics*. 2018;34(17):i884–i890.

Cox RM. Sex steroids as mediators of phenotypic integration, genetic correlations, and evolutionary transitions. *Mol Cell Endocrinol*. 2020;502:110668. doi:10.1016/j.mce.2019.110668

Cox RM, Butler MA, John-Alder HB. The evolution of sexual size dimorphism in reptiles. In: Fairbairn DJ, Blanckenhorn WU, Szekely T, editors. *Sex, size and gender roles: evolutionary studies of sexual size dimorphism*. Chapter 4. Oxford: Oxford University Press; 2007. p. 38–49.

Cox RM, Cox CL, McGlothlin JW, Card DC, Andrew AL, Castoe TA. Hormonally mediated increases in sex-biased gene expression accompany the breakdown of between-sex genetic correlations in a sexually dimorphic lizard. *Am Nat*. 2017;189(3):315–332.

Cox RM, Hale MD, Wittman TN, Robinson CD, Cox CL. Evolution of hormone-phenotype couplings and hormone-genome interactions. *Horm Behav*. 2022;144:105216. doi:10.1016/j.yhbeh.2022.105216

Cox CL, Hanninen AF, Reedy AM, Cox RM. Female anoles retain responsiveness to testosterone despite the evolution of androgen-mediated sexual dimorphism. *Funct Ecol*. 2015;29(6):758–767.

Cox RM, John-Alder HB. Testosterone has opposite effects on male growth in lizards (*Sceloporus* spp.) with opposite patterns of sexual size dimorphism. *J Exp Biol*. 2005;208(24):4679–4687.

Cox RM, John-Alder HB. Increased mite parasitism as a cost of testosterone in male striped plateau lizards *Sceloporus virgatus*. *Funct Ecol*. 2007;21(2):327–334.

Cox RM, Skelly SL, John-Alder HB. Testosterone inhibits growth in juvenile male eastern fence lizards (*Sceloporus undulatus*): implications for energy allocation and sexual size dimorphism. *Physiol Biochem Zool*. 2005b;78(4):531–545.

Cox RM, Skelly SL, Leo A, John-Alder HB. Testosterone regulates sexually dimorphic coloration in the eastern fence lizard, *Sceloporus undulatus*. *Copeia*. 2005a;2005(3):597–608.

Cox RM, Stenquist DS, Calsbeek R. Testosterone, growth, and the evolution of sexual size dimorphism. *J Evol Biol*. 2009;22(8):1586–1598.

Cox RM, Zilberman V, John-Alder HB. Testosterone stimulates the expression of a social color signal in Yarrow's spiny lizard, *Sceloporus jarrovii*. *J Exp Zool A: Ecol Genet Physiol*. 2008;309(9):505–514.

Dadras SS, Cai X, Abasolo I, Wang Z. Inhibition of 5α-reductase in rat prostate reveals differential regulation of androgen-response gene expression by testosterone and dihydrotestosterone. *Gene Expr*. 2001;9(4–5):183–194.

Enbody EK, Sin SYW, Boersma J, Edwards SV, Ketaloya S, Schwabl H, Webster MS, Karubian J. The evolutionary history and mechanistic basis of female ornamentation in a tropical songbird. *Evolution*. 2022;76(8):1720–1736.

Frankl-Vilches C, Kuhl H, Werber M, Klages S, Kerick M, Bakker A, de Oliveria EHC, Reusch C, Capuano F, Vowinckel J, et al. Using the canary genome to decipher the evolution of hormone-sensitive gene regulation in seasonal singing birds. *Genome Biol*. 2015;16(1):1–25.

Fricker LD, McKinzie AA, Sun J, Curran E, Qian Y, Yan L, Patterson SD, Courchesne PL, Richards B, Levin N, et al. Identification and characterization of proSAAS, a granin-like neuroendocrine peptide precursor that inhibits prohormone processing. *J Neurosci*. 2000;20(2):639–648.

Fuxjager MJ, Eaton J, Lindsay WR, Salwiczek LH, Rensel MA, Barske J, Sorenson L, Day LB, Schlinger BA. Evolutionary patterns of adaptive acrobatics and physical performance predict expression profiles of androgen receptor—but not oestrogen receptor—in forelimb musculature. *Funct Ecol*. 2015;29(9):1197–1208.

Fuxjager MJ, Schuppe ER. Androgenic signaling systems and their role in behavioral evolution. *J Steroid Biochem Mol Biol*. 2018;184:47–56. doi:10.1016/j.jsbmb.2018.06.004

Gazda MA, Araújo PM, Lopes RJ, Toomey MB, Andrade P, Afonso S, Marques C, Nunes L, Pereira P, Trigo S, et al. A genetic mechanism for sexual dichromatism in birds. *Science*. 2020;368(6496):1270–1274.

Gompel N, Prud'homme B, Wittkopp PJ, Kassner VA, Carroll SB. Chance caught on the wing: *cis*-regulatory evolution and the origin of pigment patterns in *Drosophila*. *Nature*. 2005;433(7025):481–487.

Hale MD, Robinson CD, Cox CL, Cox RM. Ontogenetic change in male expression of testosterone-responsive genes contributes to the emergence of sex-biased gene expression in *Anolis sagrei*. *Front Physiol*. 2022;13:886973. doi:10.3389/fphys.2022.886973

Harno E, Ramamoorthy TG, Coll AP, White A. POMC: the physiological power of hormone processing. *Physiol Rev*. 2018;98(4):2381–2430.

Hau M. Regulation of male traits by testosterone: implications for the evolution of vertebrate life histories. *Bioessays*. 2007;29(2):133–144.

Hews DK, Hara E, Anderson MC. Sex and species differences in plasma testosterone and in counts of androgen receptor-positive cells in key brain regions of *Sceloporus* lizard species that differ in aggression. *Gen Comp Endocrinol*. 2012;176(3):493–499.

Horton BM, Hudson WH, Ortlund EA, Shirk S, Thomas JW, Young ER, Zinzow-Kramer WM, Maney DL. Estrogen receptor α polymorphism in a species with alternative behavioral phenotypes. *Proc Natl Acad Sci USA*. 2014;111(4):1443–1448.

Huang Y, Shang R, Lu G-A, Zeng W, Huang C, Zou C, Tang T. Spatiotemporal regulation of a single adaptively evolving *trans*-regulatory element contributes to spermatogenetic expression divergence in *Drosophila*. *Mol Biol Evol*. 2022;39(7):msac127.

Hughes JT, Williams ME, Rebeiz M, Williams TM. Widespread *cis*- and *trans*-regulatory evolution underlies the origin, diversification, and loss of a sexually dimorphic fruit fly pigmentation trait. *J Exp Zool B: Mol Dev Evol*. 2023;340(2):143–161. doi:10.1002/jez.b.23068

Husak JF, Lovern MB. Variation in steroid hormone levels among Caribbean *Anolis* lizards: endocrine system convergence? *Horm Behav*. 2014;65(4):408–415.

Jiménez-Arcos VH, Sanabria-Urbán S, Cueva del Castillo R. The interplay between natural and sexual selection in the evolution of sexual size dimorphism in *Sceloporus* lizards (Squamata: Phrynosomatidae). *Ecol Evol*. 2017;7(3):905–917.

Jin Y, Tong H, Shao G, Li J, Lv Y, Wo Y, Brown RP, Fu C. Dorsal pigmentation and its association with functional variation in *MC1R* in a lizard from different elevations on the Qinghai-Tibetan Plateau. *Genome Biol Evol*. 2020;12(12):2303–2313.

John-Alder HB, Cox RM. Development of sexual size dimorphism in lizards: testosterone as a bipotential growth regulator. In: Fairbairn DJ, Szekely T, Blanckenhorn WU, editors. *Sex, size and gender roles: evolutionary studies of sexual size dimorphism*. Oxford: Oxford University Press; 2007. p. 195–204.

John-Alder HB, Cox RM, Haenel GJ, Smith LC. Hormones, performance and fitness: natural history and endocrine experiments on a lizard (*Sceloporus undulatus*). *Integr Comp Biol*. 2009;49(4):393–407.

Johnson MJ, Kircher BK, Castro DJ. The evolution of androgen receptor expression and behavior in *Anolis* lizard forelimb muscles. *J Comp Physiol A*. 2018;204(1):71–79.

Kelsh RN, Brand M, Jiang Y-J, Heisenberg C-P, Lin S, Haffter P, Odenthal J, Mullins MC, van Eeden FJM, Furutani-Seiki M, et al. Zebrafish pigmentation mutations and the processes of neural crest development. *Development*. 1996;123(1):369–389.

Kelsh RN, Schmid S, Eisen JS. Genetic analysis of melanophore development in zebrafish embryos. *Dev Biol*. 2000;225(2):277–293.

Ketterson ED, Atwell JW, McGlothlin JW. Phenotypic integration and independence: hormones, performance, and response to environmental change. *Integr Comp Biol*. 2009;49(4):365–379.

Khalil S, Welklin JF, McGraw KJ, Boersma J, Schwabl H, Webster MS, Karubian J. Testosterone regulates *CYP2J19*-linked carotenoid signal expression in male red-backed fairywrens (*Malurus melanocephalus*). *Proc R Soc Lond B: Biol Sci*. 2020;287(1935):20201687.

Kimball FA, Erpino MJ. Hormonal control of pigmentary sexual dimorphism in *Sceloporus occidentalis*. *Gen Comp Endocrinol*. 1971;16(2):375–384.

King RA, Pietsch J, Fryer JP, Savage S, Brott MJ, Russell-Eggitt I, Summers CG, Oetting WS. Tyrosinase gene mutations in oculocutaneous albinism 1 (OCA1): definition of the phenotype. *Hum Genet*. 2003;113:502–513. doi:10.1007/s00439-003-0998-1

Klaassen H, Wang Y, Adamski K, Rohner N, Kowalko JE. CRISPR mutagenesis confirms the role of *oca2* in melanin pigmentation in *Astyanax mexicanus*. *Dev Biol*. 2018;441(2):313–318.

Kobayashi T, Imokawa G, Bennett DC, Hearing VJ. Tyrosinase stabilization by Tyrp1 (the *brown* locus protein). *J Biol Chem*. 1998;273(48):31801–31805.

Koshikawa S. Evolution of wing pigmentation in *Drosophila*: diversity, physiological regulation, and *cis*-regulatory evolution. *Dev Growth Differ*. 2020;62(5):269–278.

Koshikawa S, Giorgianni MW, Vaccaro K, Kassner VA, Yoder JH, Werner T, Carroll SB. Gain of *cis*-regulatory activities underlies novel domains of *wingless* gene expression in *Drosophila*. *Proc Natl Acad Sci USA*. 2015;112(24):7524–7529.

Kratochwil CF, Liang Y, Gerwin J, Woltering JM, Urban S, Henning F, Machado-Schiaffino G, Hulsey CD, Meyer A. Agouti-related peptide 2 facilitates convergent evolution of stripe patterns across cichlid fish radiations. *Science*. 2018;362(6413):457–460.

Li J, Bed'hom B, Marthey S, Valade M, Dureux A, Moroldo M, Péchoux C, Coville J-L, Gourichon D, Vieaud A, et al. A missense mutation in *TYRP1* causes the chocolate plumage color in chicken and alters melanosome structure. *Pigment Cell Melanoma Res*. 2019;32(3):381–390.

Liao Y, Smyth GK, Shi W. The Subread aligner: fast, accurate and scalable read mapping by seed-and-vote. *Nucleic Acid Res*. 2013;41(10):e108.

Liao Y, Smyth GK, Shi W. featureCounts: an efficient general purpose program for assigning sequence reads to genomic features. *Bioinformatics*. 2014;30(7):923–930.

Lin T-M, Chang C. Cloning and characterization of TDD5, an androgen target gene that is differentially repressed by testosterone and dihydrotestosterone. *Proc Natl Acad Sci USA*. 1997;94(10):4988–4993.

Lipshutz SE, George EM, Bentz AB, Rosvall KA. Evaluating testosterone as a phenotypic integrator: from tissues to individuals to species. *Mol Cell Endocrinol*. 2019;496:110531. doi:10.1016/j.mce.2019.110531

Luecke D, Rice G, Kopp A. Sex-specific evolution of a *Drosophila* sensory system via interacting *cis*- and *trans*-regulatory changes. *Evol Dev*. 2022;24(1–2):37–60.

Lyons LA, Foe IT, Rah HC, Grahn RA. Chocolate coated cats: *TYRP1* mutations for brown color in domestic cats. *Mamm Genome*. 2005a;16:356–366. doi:10.1007/s00335-004-2455-4

Lyons LA, Imes DL, Rah HC, Grahn RA. Tyrosinase mutations associated with Siamese and Burmese patterns in the domestic cat (*Felis catus*). *Anim Genet*. 2005b;36(2):119–126.

Mank JE. Sex chromosomes and the evolution of sexual dimorphism: lessons from the genome. *Am Nat*. 2009;173(2):141–150.

McLean CA, Lutz A, Rankin KJ, Stuart-Fox D, Adnan M. Revealing the biochemical and genetic basis of color variation in a polymorphic lizard. *Mol Biol Evol*. 2017;34(8):1924–1935.

Merritt JR, Grogan KE, Zinzow-Kramer WM, Sun D, Ortlund EA, Yi SV, Maney DL. A supergene-linked estrogen receptor drives alternative phenotypes in a polymorphic songbird. *Proc Natl Acad Sci USA*. 2020;117(35):21673–21680.

Morrison RL, Rand MS, Frost-Mason SK. Cellular basis of color differences in three morphs of the lizard *Sceloporus undulatus erythrocheilus*. *Copeia*. 1995;1995(2):397–408.

Mort RL Jackson IJ, Patton EE. The melanocyte lineage in development and disease. *Development*. 2015;142(4):620–632.
Mundy NI. A window on the genetics of evolution: *MC1R* and plumage colouration in birds. *Proc R Soc Lond B: Biol Sci*. 2005;272(1573):1633–1640.
Nachman MW, Hoekstra HE, D'Agostino SL. The genetic basis of adaptive melanism in pocket mice. *Proc Natl Acad Sci USA*. 2003;100(9):5268–5273.
Nicolaï MPJ, D'Alba L, Goldenberg J, Gansemans Y, Van Nieuwerburgh F, Clusella-Trullas S, Shawkey MD. Untangling the structural and molecular mechanisms underlying colour and rapid colour change in a lizard, *Agama atra*. *Mol Ecol*. 2021;30(10):2262–2284.
Oetting WS, Savage Garrett S, Brott M, King RA. P gene mutations associated with oculocutaneous albinism II (OCA2). *Hum Mutat*. 2005;25(3):323–329.
Ossip-Drahos AG, Oyola Morales JR, Vital-García C, Zúñiga-Vega JJ, Hews DK, Martins EP. Shaping communicative colour signals over evolutionary time. *R Soc Open Sci*. 2016;3(11):160728.
Parichy DM. Evolution of pigment cells and patterns: recent insights from teleost fishes. *Curr Opin Genet Dev*. 2021;69:88–96. doi:10.1016/j.gde.2021.02.006
Parichy DM, Rawls JF, Pratt SJ, Whitfield TT, Johnson SL. Zebrafish *sparse* corresponds to an orthologue of *c-kit* and is required for the morphogenesis of a subpopulation of melanocytes, but is not essential for hematopoiesis or primordial germ cell development. *Development*. 1999;126(15):3425–3436.
Park HY, Kosmadaki M, Yaar M, Gilchrest BA. Cellular mechanisms regulating human melanogenesis. *Cell Mol Life Sci*. 2009;66:1493–1506. doi:10.1007/s00018-009-8703-8
Passmore LA, Kaesmann-Kellner B, Weber BHF. Novel and recurrent mutations in the tyrosinase gene and the P gene in the German albino population. *Hum Genet*. 1999;105:200–210. doi:10.1007/s004399900104
Phipson B, Lee S, Majewski IJ, Alexander ES, Smyth GK. Robust hyperparameter estimation protects against hypervariable genes and improves power to detect differential expression. *Ann Appl Stat*. 2016;10(2):946–963.
Pollock NB, Feigin S, Drazenovic M, John-Alder HB. Sex hormones and the development of sexual size dimorphism: 5α-dihydrotestosterone inhibits growth in a female-larger lizard (*Sceloporus undulatus*). *J Exp Biol*. 2017;220(21):4068–4077.
Prud'homme B, Gompel N, Carroll SB. Emerging principles of regulatory evolution. *Proc Natl Acad Sci USA*. 2007;104(suppl_1):8605–8612.
Prud'homme B, Gompel N, Rokas A, Kassner VA, Williams TM, Yeh S-D, True JR, Carroll SB. Repeated morphological evolution of *cis*-regulatory changes in a pleiotropic gene. *Nature*. 2006;440(7087):1050–1053.
Qian Y, Devi LA, Mzhavia N, Munzer S, Seidah NG, Fricker LD. The C-terminal region of proSAAS is a potent inhibitor of prohormone convertase 1. *J Biol Chem*. 2000;275(31):23596–23601.
Quigley IK, Turner JM, Muckels RJ, Manuel JL, Budi EH, MacDonald EL, Parichy DM. Pigment pattern evolution by differential deployment of neural crest and post-embryonic melanophore lineages in *Danio* fishes. *Development*. 2004;131(24):6053–6069.
Quinn VS, Hews DK. Positive relationship between abdominal coloration and dermal melanin density in phrynosomatid lizards. *Copeia*. 2003;2003(4):858–864.
R Core Team. *R: a language and environment for statistical computing*. Vienna (Austria): R Foundation for Statistical Computing; 2022.
Raper HS. The aerobic oxidases. *Physiol Rev*. 1928;8(2):245–282.
Reynkens T. *rospca: robust sparse PCA using ROSPCA algorithm. R package version 1.0.4*. 2018.
Rinn JL, Snyder M. Sexual dimorphism in mammalian gene expression. *Trends Genet*. 2005;21(5):298–305.
Robinson CD, Gifford ME. Intraseasonal changes of patch color in prairie lizards (*Sceloporus consobrinus*). *Herpetologica*. 2019;75(1):79–84.
Robinson MD, McCarthy DJ, Smyth GK. edgeR: a Bioconductor package for differential expression analysis of digital gene expression data. *Bioinformatics*. 2010;26(1):139–140.
Rosenblum EB, Hoekstra H, Nachman MW. Adaptive reptile color variation and the evolution of the *MC1R* gene. *Evolution*. 2004;58(8):1794–1808.
Rosenblum EB, Römpler H, Schöneberg T, Hoekstra HE. Molecular and functional basis of phenotypic convergence in white lizards at White Sands. *Proc Natl Acad Sci USA*. 2010;107(5):2113–2117.
Rosvall KA, Burns CMB, Jayaratna SP, Ketterson ED. Divergence along the gonadal steroidogenic pathway: implications for hormone-mediated phenotypic evolution. *Horm Behav*. 2016;84:1–8. doi:10.1016/j.yhbeh.2016.05.015
Rousseau K, Kauser S, Pritchard LE, Warhurst A, Oliver RL, Slominski A, Wei ET, Thody AJ, Tobin DJ, White A. Proopiomelanocortin (POMC), the ACTH/melanocortin precursor, is secreted by human epidermal keratinocytes and melanocytes and stimulates melanogeneis. *FASEB J*. 2007;21(8):1844–1856.
Sackton TB, Grayson P, Cloutier A, Hu Z, Liu JS, Wheeler NE, Gardner PP, Clarke JA, Baker AJ, Clamp M, et al. Convergent regulatory evolution and loss of flight in paleognathous birds. *Science*. 2019;364(6435):74–78.
Schartl M, Larue L, Goda M, Bosenberg MW, Hashimoto H, Kelsh RN. What is a vertebrate pigment cell? *Pigment Cell Melanoma Res*. 2016;29(1):8–14.
Schartl A, Schartl MS, Anders F. Promotion and regression of neoplasia by testosterone-promoted cell differentiation in *Xiphophorus* and *Girardinus*. *Carcinogenesis*. 1982;7:427–434.
Schauer E, Trautinger F, Köck A, Schwarz A, Bhardwaj R, Simon M, Ansel JC, Schwarz T, Luger TA. Proopiomelanocortin-derived peptides are synthesized and released by human keratinocytes. *J Clin Investig*. 1994;93(5):2258–2262.
Schindelin J, Arganda-Carreras I, Frise E, Kaynig V, Longair M, Pietzsch T, Peribisch S, Rueden C, Saalfeld S, Schmid S, et al. Fiji: an open-source platform for biological-image analysis. *Nat.? Methods*. 2012;9(7):676.
Steel KP, Davidson DR, Jackson IJ. TRP-2/DT, a new early melanoblast marker, shows that steel growth factor (c-kit ligand) is a survival factor. *Development*. 1992;115(4):1111–1119.
Taylor JD, Hadley ME. Chromatophores and color change in the lizard, *Anolis carolinensis*. *Z Zellforsch Mikrosk Anat*. 1970;104(2):282–294.
The Gene Ontology Consortium. The gene ontology resource: enriching a GOld mine. *Nucleic Acid Res*. 2021;49(D1):D325–D334.
Toyofuku K, Wada I, Valencia JC, Kushimoto T, Ferrans VJ, Hearing VJ. Oculocutaneous albinism types 1 and 3 are ER retention diseases: mutation of tyrosinase or Tyrp1 can affect the processing of both mutant and wild-type proteins. *FASEB J*. 2001;15(12):2149–2161.
van Nas A, GuhaThakurta D, Wang SS, Yehya N, Horvath S, Zhang B, Ingram-Drake L, Chaudhuri G, Schadt EE, Drake TA, et al. Elucidating the role of gonadal hormones in sexually dimorphic gene coexpression networks. *Endocrinology*. 2009;150(3):1235–1249.
Waxman DJ, O'Connor C. Growth hormone regulation of sex-dependent liver gene expression. *Mol Endocrinol*. 2006;20(11):2613–2629.
Werner T, Koshikawa S, Williams TM, Carroll SB. Generation of a novel wing colour pattern by the Wingless morphogen. *Nature*. 2010;464(7292):1143–1148.
West-Eberhard MJ. 2003. *Developmental plasticity and evolution*. New York: Oxford University Press.
Westfall AK, Telemeco RS, Grizante MB, Waits DS, Clark AD, Simpson DY, Klabacka RL, Sullivan AP, Perry GH, Sears MW, et al. A chromosome-level genome assembly for the eastern fence lizard (*Sceloporus undulatus*), a reptile model for physiological and evolutionary ecology. *GigaScience*. 2021;10(10):giab066.
Wiens JJ. Phylogenetic evidence for multiple losses of a sexually selected character in phrynosomatid lizards. *Proc R Soc Lond B: Biol Sci*. 1999;266(1428):1529–1535.

Williams TM, Carroll SB. Genetic and molecular insights into the development and evolution of sexual dimorphism. *Nat Rev Genet*. 2009;10(11):797–804.

Wintzen M, Yaar M, Burbach JPH, Gilchrest BA. Proopiomelanocortin gene product regulation in keratinocytes. *J Investig Dermatol*. 1996;106(4):673–678.

Wittkopp PJ, Kalay G. *Cis*-regulatory elements: molecular mechanisms and evolutionary processes underlying divergence. *Nat Rev Genet*. 2012;13(1):59–69.

Wittman TN, Robinson CD, McGlothlin JW, Cox RM. Hormonal pleiotropy structures genetic covariance. *Evol Lett*. 2021;5(4):397–407.

Wright AE, Rogers TF, Fumagalli M, Cooney CR, Mank JE. Phenotypic sexual dimorphism is associated with genomic signatures of resolved sexual conflict. *Mol Ecol*. 2019;28(11):2860–2871.

Xu X, Coats JK, Yang CF, Wang A, Ahmed OM, Alvarado M, Izumi T, Shah NM. Modular genetic control of sexually dimorphic behaviors. *Cell*. 2012;148(3):596–607.

Yokoyama T, Silversides DW, Waymire KG, Kwon BS, Takeuchi T, Overbeek PA. Conserved cysteine to serine mutation in tyrosinase is responsible for the classical albino mutation in laboratory mice. *Nucleic Acids Res*. 1990;18(24):7293–7298.

Zeileis A, Hothorn T. Diagnostic checking in regression relationships. *R News*. 2002;2(3):7–10.